

Macrovoids formation and light scattering of PMMA

ZHI HONG CHEN, Z C CHANG[†] and C B LIN^{*}

Department of Mechanical and Electro-mechanical Engineering, Tamkang University, Tamsui, Taipei County, Republic of China

[†]Department of Mechanical Engineering, National Chin-Yi Institute of Technology, Taiping City, Taichung County, Republic of China

MS received 24 January 2007; revised 6 March 2007

Abstract. After desorption of PMMA with saturated methanol and ethanol and then desorption by distilled water, the macrovoids are formed because of the phase inversion. The macrovoids on the surface of the specimens are larger and more numerous than those in the bulk. The macrovoids are likely to be closed-type, if the hydrolysis temperature is lower. On the other hand, if the hydrolysis temperature is higher, the macrovoids are likely to be open-type. Due to the formation of macrovoids, smaller than visible wavelengths, the light will disperse, and therefore, reduces the transmittance of the specimens. The transmittance is decreased when the hydrolysis temperature and hydrolysis time are increased. Furthermore, it is much clearer when ethanol is used as solvent than methanol. The scattered intensity of the specimens after hydrolysis is inversely proportional to the visible wavelength with an exponent, n , in the range 0.04–2.83 for methanol and 0.02–0.21 for ethanol.

Keywords. PMMA; hydrolysis; macrovoids; transmittance; scattering.

1. Introduction

PMMA, normally transparent, turns opaque after absorbing ethanol according to Lin *et al* (1992). The degree of opacity depends on the amount absorbed. Cleavage plane observation shows that loss in transmittance and formation of macrovoids are directly related. Incident visible lights tend to be reflected by macrovoids of size greater than the wavelength and they tend to be scattered by macrovoids of smaller dimensions. The transmittance seems to vary with the wavelength. Light scattering and fractal principles have been used in some studies (Orbach 1986; Buczkowski *et al* 1998) to investigate irregular profiles and agglomerate patterns and sizes. According to Chou and Lee (2000), the transmittance decreases as macrovoids grow bigger in size when critical amount of solvent is absorbed. Besides, the solvent absorption rate vs specimen transmittance relationship can be segmented into two to three linear transitions. The first transition occurs at the crossover in the middle of the specimen where the two swelling interfaces inter-penetrate. The second transition occurs only in specimens with low concentration of absorbed solvent. The transmittance increases initially, but then it starts decreasing as absorption continues. The swelled macrovoids can be deemed as scattering particles in the specimen. In this light, the specimen's treatment in solvent binds the specimen's transmittance

to a fixed relationship with the wavelength of the incident light. The light scattering intensity is inversely proportional to the n th power of the incident wavelength, where n varies from 1.2–3.26. For Rayleigh scattering, viz. surface scattering, $n = 4$ (Jenkins and White 1950). The deviation from Rayleigh index implies that the macrovoids possess the dimension of a fractal. In addition, residual composite solvent particles in the specimen also scatter lights and affect the index, n .

The first part of the study is to make the macrovoids form in PMMA by hydrolysis process at elevated temperatures following the saturation of PMMA by methanol and ethanol, and distilled water as extractor. The effects of hydrolysis temperature and hydrolysis time on the macrovoids formation mechanism and the macrovoids morphology are also investigated. In the second part of the study, relationships between the transmittance of the membrane and the wavelength of the incident light are also discussed.

2. Experimental

2.1 Specimen preparation

The polymer specimen was PMMA with an intrinsic viscosity of 0.237 dl/g from Du Pont in the form of a 0.25" thick Lucite L type cast acrylic sheet, which was cut into 50 × 20 × 1 mm² pieces. The grades of methanol and ethanol used were from J. T. Baker Co. Ltd. and Ridel-DeHaen Co. Ltd., respectively.

*Author for correspondence (cblin@mail.tku.edu.tw)

2.2 Solvent adsorption and hydrolysis

The PMMA specimens and the solvent were pre-heated to the working temperature of 60°C and the specimens were immersed into the solvent. The specimens were taken out periodically to be weighed with a microbalance (± 0.1 mg) until saturated adsorption was reached. The working temperature was set at 60°C since the boiling temperature of methanol is 65°C and we did not want any vapourization to take place during the absorption process.

After saturated absorption, one batch of the specimens was rapidly immersed in 40–80°C distilled water for hydrolysis for 3 h and another batch in 60°C distilled water for 0.5–4 h, respectively. These specimens were then taken out of the hydrolysis system for 24 h hydrolysis in the atmosphere until the weight no longer changed. For the purpose of understanding the interaction between the absorbed solvent and distilled water during hydrolysis, a third batch of the specimens was placed in 25°C atmosphere and in 40–80°C distilled water for hydrolysis, respectively. These samples were carefully weighed with a digital balance during the hydrolysis procedure until the weight ceased to change. Hydrolysis temperature was kept at 40–80°C for two reasons: PMMA cannot produce macrovoids at a hydrolysis temperature below 30°C for one and PMMA will deform at a hydrolysis temperature of above 80°C for the other.

2.3 SEM analysis

A completely hydrolyzed specimen was cleaved for this purpose. A notch was scribed on the specimen's surface at the centre and it was then aligned with the blade bottom on the pincers. An external force was applied so that the crack propagated along the notch. The purpose of the notch was to produce a fracture surface of the brittle fracture type. The morphology of the cleaved surface was observed with a LEO-1530 scanning electron microscope (SEM). About 2.5 nm Au in thickness was sputtered on the cleaved surface before SEM observation.

2.4 Spectrum test

Transmittance of the specimens was measured in visible light range (390 ~ 780 nm) with a Hitachi U-3410/U3420 spectrometer. The scanning rate was 120 nm/min.

2.5 DSC analysis

The effective glass transition temperature of PMMA after solvent absorption was analysed with a SEIKO 1 SSC-5000 DSC. The specimen was immersed in either methanol or ethanol until saturation at 60°C. Each saturated specimen, weighing about 10 mg, was enclosed in a regular aluminum pan and moved into the DSC. The aluminum

pan was sealed to keep the solvent inside the PMMA specimen from evaporating. The sample was heated from room temperature to 105°C with a heating rate of 5°C/min.

3. Results and discussion

3.1 Mass transport behaviour

Mass transport in PMMA was conducted at 60°C in methanol and ethanol, respectively. Variation of the absorbed solvent vs mass transport time, $M_t/M_0 \times 100\%$, is shown in figure 1, where M_0 represents the weight of the virgin specimen before solvent absorption, and M_t represents the weight of the specimen at absorption time, t . The solid line in figure 1 is plotted through curve fitting of the experimental data using the mathematical model proposed by Harmon *et al* (1987, 1988) that represents mass transport through anomalous diffusion. The model captures the fundamentals of concentration gradient and flux in the solvent transport mass-time characteristics in a finite-thickness, symmetric system. The equation for the same is as follows:

$$\frac{M_t}{M_\infty} = 1 - 2 \sum_{n=1}^{\infty} \frac{\lambda_n^2 (1 - 2 \cos \lambda_n) \exp\left(\frac{-v l}{2D}\right)}{\beta_n^4 \left(1 - \frac{2D}{v l} \cos^2 \lambda_n\right)} \exp\left(-\beta_n^2 \frac{D t}{l^2}\right), \quad (1)$$

$$\lambda_n = \frac{v l}{2D} \tan \lambda_n \rightarrow \beta_n^2 = \frac{v^2 l^2}{4D^2} + \frac{v^2 l^2}{4D^2} \tan^2 \lambda_n, \quad (2)$$

$$\beta_n^2 = \frac{v^2 l^2}{4D^2} + \lambda_n^2 \rightarrow \cos^2 \lambda_n = \frac{v^2 l^2}{4D^2 \beta_n^2}, \quad (3)$$

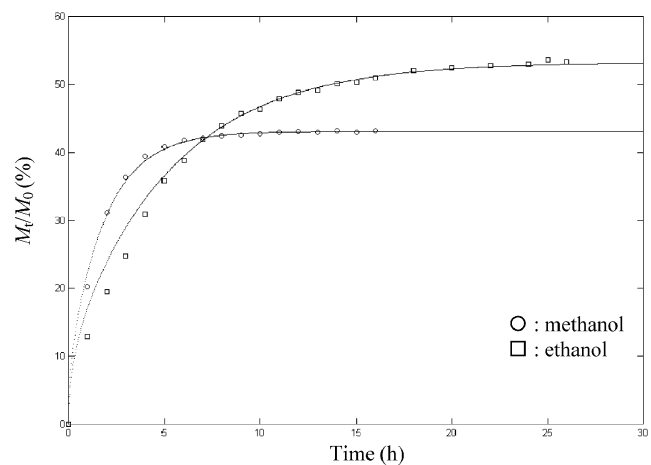


Figure 1. Amount of solvent absorption ($M_t/M_0 \times 100\%$) vs mass transport time when the PMMA specimen was mass transported in 60°C methanol and ethanol.

Table 1. The equilibrium coefficients of PMMA after absorbing methanol and ethanol. The diffusion coefficient (D) and velocity (v) are included. ESC represents the amount of saturated solvent absorption, and T_{geff} represents the effective glass transition temperature.

Solvent	Solubility (cal/cm^3) ^{1/2}	Boiling temperature ($^{\circ}\text{C}$)	$D \times 10^8$ (cm^2/s)	$v \times 10^6$ (cm/s)	ESC (wt%)	T_{geff} ($^{\circ}\text{C}$)
Methanol	14.3	64.7	11.1	8.9	43.05	23.2
Ethanol	12.9	78.2	4.1	5.7	53.26	18.7

The solubility parameter of PMMA: 9.2.

where M_t is the amount of weight gained in the specimen after absorption time, t , M_{∞} the amount of weight gained after the absorption reaches saturation, D the diffusion coefficient due to random walk of the solvent molecules in case I, v the velocity due to stress relaxation of the polymer chain in case II, $2l$ the thickness of the specimen, and λ_n will always be positive real part of the solution that satisfies (2) and (3).

Table 1 shows the coefficients at equilibrium for PMMA that is saturated by methanol and ethanol. The diffusion coefficient (D) in case I and the velocity (v) in case II are included. ESC is the equilibrium solvent content of the system, which is defined as the weight of the solvent in the specimen at equilibrium divided by the weight of the virgin specimen. It is known from table 1 that the diffusion coefficient and the velocity are greater in the methanol system than those in ethanol. This means that the time to reach saturation is faster in the methanol system than in ethanol. Besides, ESC is greater in the ethanol system than in methanol. The reason is that the solubility parameter in the ethanol system is closer to PMMA than the methanol system as is shown in table 1.

The glass transition temperature of PMMA in this study is 104°C without solvent treatment. The following DSC test was used to confirm that the glass transition temperature was reduced as a result of solvent transport. PMMA specimens saturated by methanol and ethanol at different temperatures were put into the aluminum pan of the DSC to determine their effective glass transition temperature. It can be seen in table 1 that the effective glass transition temperature was always lower than the solvent treatment temperature. Additionally, the effective glass transition temperature increased with decreasing temperature of solvent treatment and the increase was steeper with ethanol as the solvent as opposed to methanol.

3.2 Hydrolysis

Weight loss of the methanol and ethanol saturated PMMA specimens during hydrolysis in $40\text{--}80^{\circ}\text{C}$ distilled water are shown in figures 2(a) and (b). Weight loss during hydrolysis under 25°C atmosphere is shown in figure 2(c). The hydrolysis behaviour in distilled water and in atmosphere were very different. In atmosphere, the weight loss slowed down quickly with hydrolysis time and reached

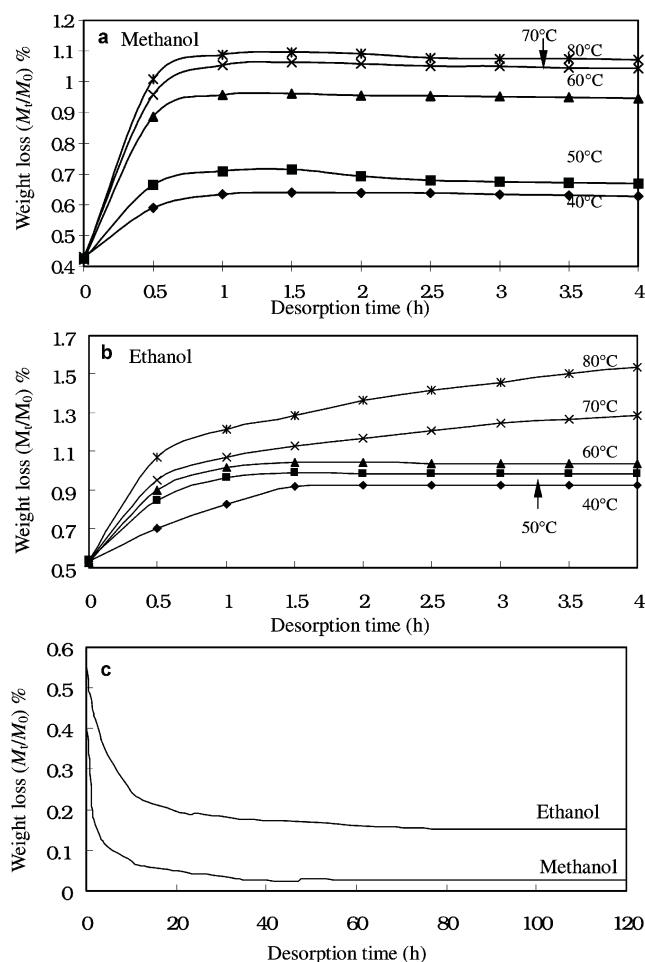


Figure 2. Hydrolysis curves for PMMA with saturated methanol and ethanol at 60°C and then hydrolyzed in $40\text{--}80^{\circ}\text{C}$ distilled water or in 25°C atmosphere: a. in the methanol system, b. in the ethanol system and c. in 25°C atmosphere.

an equilibrium state eventually. The initial hydrolysis rate was faster in the methanol system than in ethanol. In distilled water, on the other hand, there was weight gain rather than weight loss with time. In the methanol system, the amount of weight gain increased with both hydrolysis temperature and hydrolysis time. But the rate slowed down with time and saturation was reached eventually when the weight stopped changing. One reason is that, as the solvent is hydrolyzed from the inside of the specimen to

the outside, the solvent is impeded by distilled water. Another reason is that, as the effective glass transition temperature of PMMA is lowered, as shown in table 1, the amount of distilled water diffusing into the PMMA specimen increases. But as the hydrolysis process continues, the effective glass transition temperature of PMMA gradually recovers and water diffusion slows down. When it is eventually elevated to above the hydrolysis temperature, water diffusion stops and no further weight gain is seen. As to the ethanol system, since there is more solvent absorption and the correspondent effective glass transition temperature is much lower, as shown in table 1, the window for mass transport of water into PMMA is wider, allowing more distilled water to enter the specimen.

Volume expansion rate, density and void ratio after hydrolysis in distilled water for 3 h at 40–80°C are shown in table 2, where volume expansion rate ($(V-V_0)/V_0$) is the change in volume after hydrolysis divided by the volume of the virgin specimen and void ratio ($(\rho_0 - \rho/\rho_0) \times 100\%$) is the change in density after hydrolysis divided by the

density of the virgin specimen. Both volume expansion rate and void ratio increased with the hydrolysis temperature and the amount of increase was larger in the ethanol system than in methanol.

3.3 Microstructure

The SEM micrograph of the cleavage surface of the PMMA specimen pre-saturated by methanol at 60°C and hydrolyzed in 60°C distilled water for 0.5 h is shown in figure 3(a). Elliptic macrovoids were formed along both sides of the specimen. The major axis and the minor axis of the elliptic macrovoids was about 200 μm and 100 μm , respectively. The major axis was parallel to the direction of solvent mass transport. Inside each elliptic macrovoid were many closed macrovoids and their number and size increased with hydrolysis time, as can be seen in figure 4. They were about 0.05 μm in size after 0.5 h hydrolysis and about 1 μm after 4 h. For comparison, magnified micrographs of the specimen's interior region are shown in figure 5. Macrovoids in the interior were also closed-type and their number and size also increased with hydrolysis time. But they were smaller in size than those inside the elliptic macrovoids.

For PMMA that were saturated by methanol at 60°C, morphology after hydrolysis in distilled water at different temperatures was also examined. At 60°C and 70°C, elliptic macrovoids were formed, as shown in figure 3(a). No elliptic macrovoids were seen at 40°C, 50°C and 80°C hydrolysis temperature. At 80°C, however, as shown in figure 6, two distinguishable layers of macrovoids, the outer and the inner, can be seen. Magnified micrographs of macrovoids inside the elliptic macrovoids after hydrolysis at 60°C and inside the outer layer at 80°C are shown in figures 7(a) and (b), respectively. Macrovoids inside the elliptic macrovoids were of the closed-type but they were sponge-like in the outer layer. Morphology for the specimen interior after hydrolysis at 40–80°C is shown in figure 8. At 40°C, no macrovoids were detectable even at 2×10^4 magnification. At 50°C and above, closed-type macrovoids were seen with their size and number increasing with the hydrolysis temperature.

Morphology of the cleavage surface of PMMA pre-saturated by ethanol at 60°C and then hydrolyzed in distilled water at 60°C for 0.5 h is shown in figure 3(b). Elliptic macrovoids were formed along the outside layer. The major axis and the minor axis of the elliptic macrovoids was about 600 μm and 300 μm , respectively. On comparing figures 3(a) and (b), at equal hydrolysis time, the elliptic macrovoids were found to be larger in ethanol than in methanol. Magnified micrographs of the macrovoids inside the elliptic macrovoids after 0.5–4 h hydrolysis time are shown in figure 9. They were of open-type. Quantitatively, the porosity increased with hydrolysis time. Magnified micrographs of the specimen interior after hydrolysis

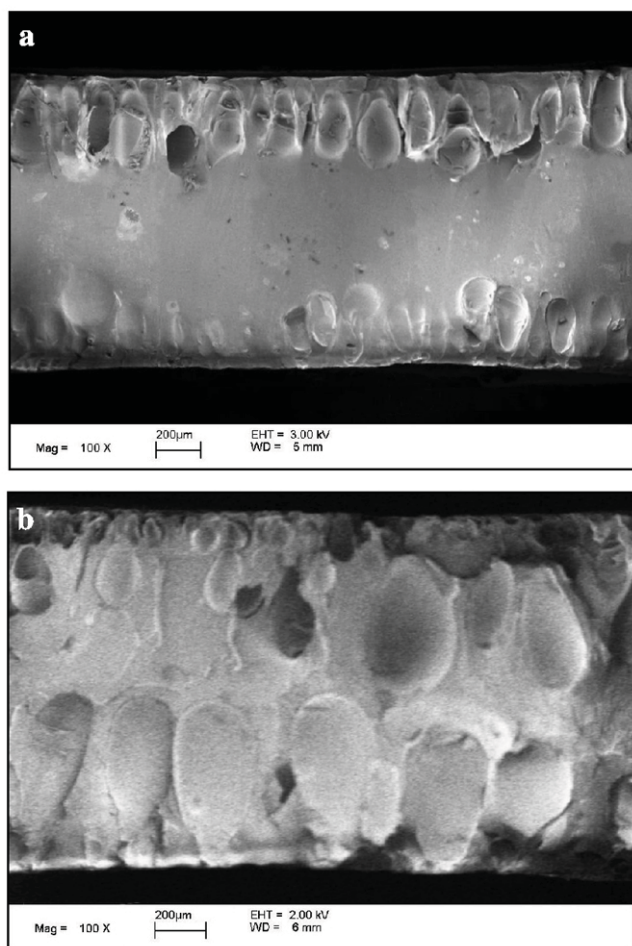


Figure 3. Morphology of the cleavage surface for PMMA pre-saturated by **a.** methanol and **b.** ethanol at 60°C, and then hydrolyzed in 60°C distilled water for 0.5 h. Elliptic macrovoids are formed along both sides of the specimen.

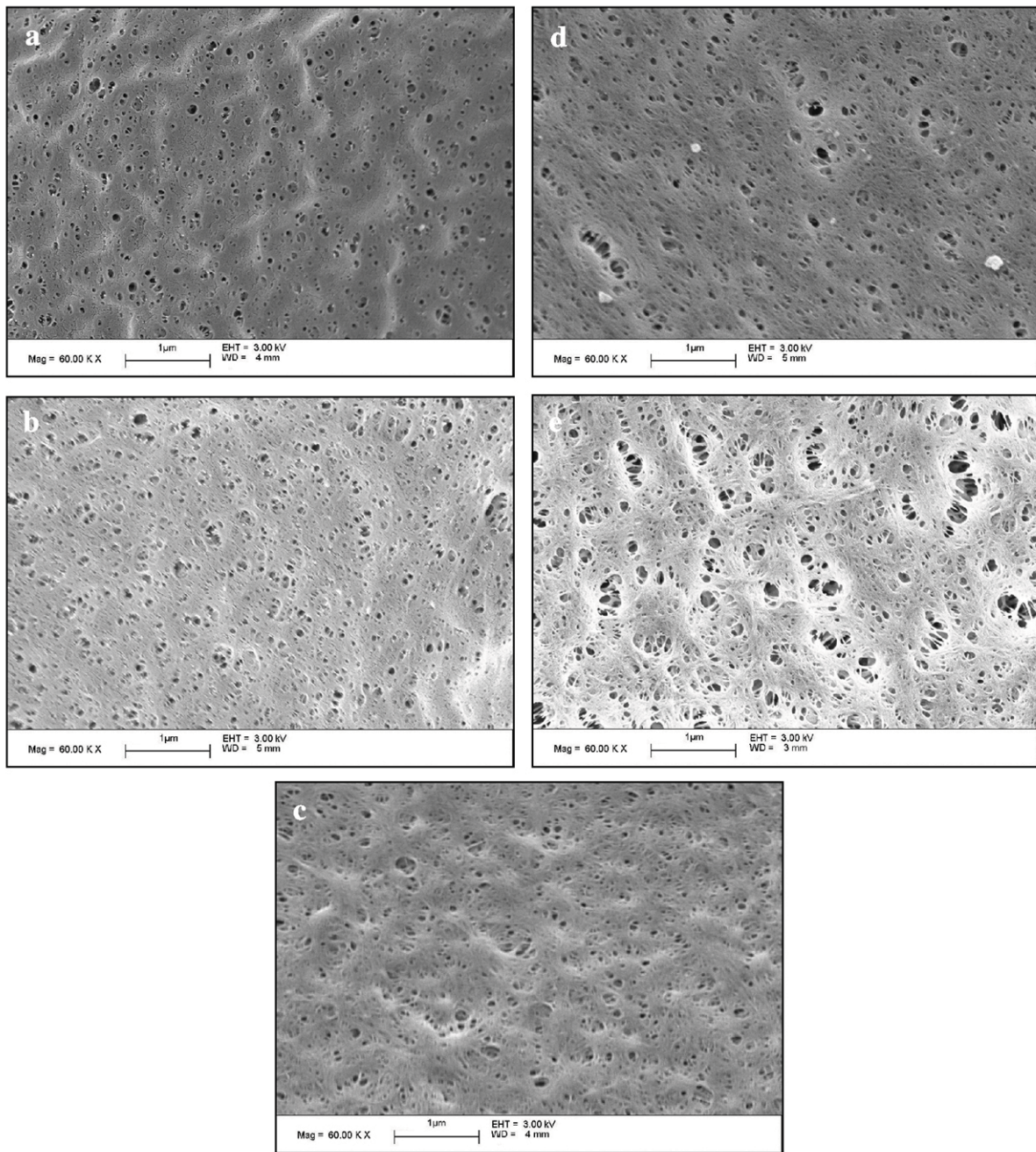


Figure 4. Magnified morphology inside the elliptic macrovoids for PMMA with saturated methanol at 60°C and then hydrolyzed in 60°C distilled water for **a.** 0.5 h, **b.** 1 h, **c.** 2 h, **d.** 3 h and **e.** 4 h hydrolysis time.

for 0.5–4 h are shown in figure 10. The macrovoids were closed-type and their size and number also increased with hydrolysis time. By comparing figure 4 with figure 9, it was found that the macrovoids inside the elliptic macrovoids were closed-type for methanol treated specimens but they were open-type for ethanol treated specimens. Macrovoids in the specimen interior, however, were both of the closed-type. By comparing figure 5 with figure 10, the closed-

type macrovoids in the specimen interior were larger in the ethanol system than in methanol.

As can be seen in figure 3(b), elliptic macrovoids were formed along the outside layer at 40–60°C hydrolysis temperature in the ethanol system. At 60°C hydrolysis, the elliptic macrovoids on both sides of the specimen were close to joining. The morphology for the macrovoids at hydrolysis temperatures 70–80°C was sponge-like, as shown in

figure 11. The morphology inside the elliptic macrovoids at hydrolysis temperature 40–60°C was of the open-type,

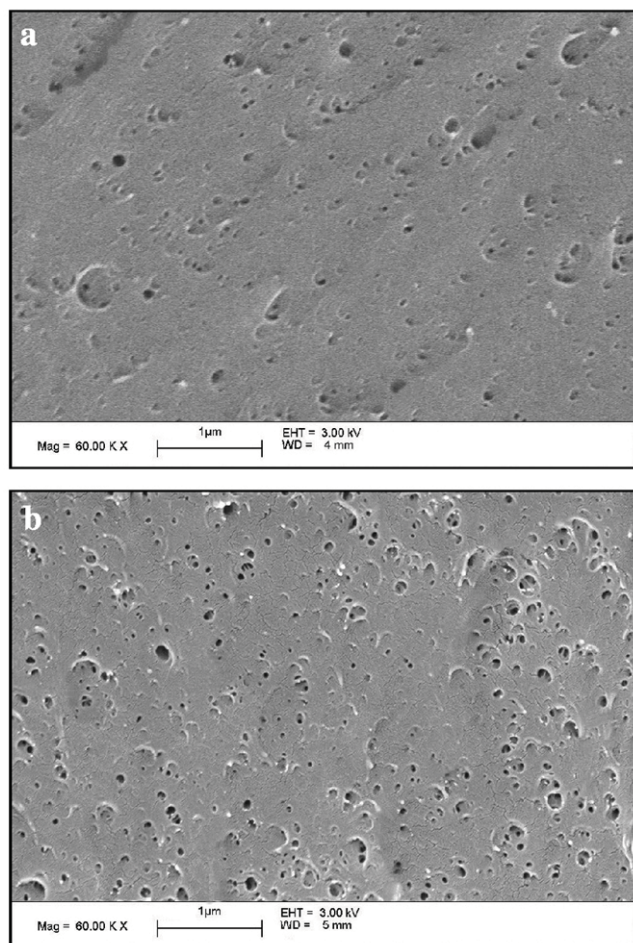


Figure 5. Morphology of the interior region of the specimen pre-saturated by methanol at 60°C and then hydrolyzed in 60°C distilled water for **a.** 0.5 h and **b.** 4 h hydrolysis time.

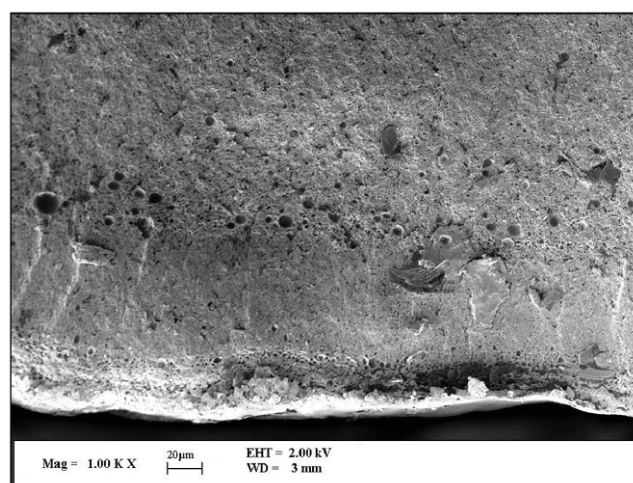


Figure 6. Morphology of the cleavage surface for PMMA saturated by methanol at 60°C and then fully hydrolyzed in 80°C distilled water.

as shown in figure 12(a), and the size increased with hydrolysis temperature. In contrast, the morphology at 70–80°C hydrolysis temperature was sponge-like, as shown in figure 12(b). For the interior, morphology at 40–80°C hydrolysis temperature is shown in figure 13. The morphology of the macrovoids from 40–60°C were closed-type and from 70–80°C were open-type. The size and number of the closed macrovoids and the porosity of the open macrovoids all increased with increasing hydrolysis temperature.

3.4 Formation mechanism of macrovoids

Upon absorbing the solvent at 60°C and then hydrolyzing in 40–80°C distilled water, the effective glass transition temperature rises back up, the organic solvent in the PMMA specimens will then diffuse outwards. Concurrently, distilled water diffuses into the PMMA, blocking some of the organic solvent from being mass-transported out of the specimen. As a result, probability exists for the solvent

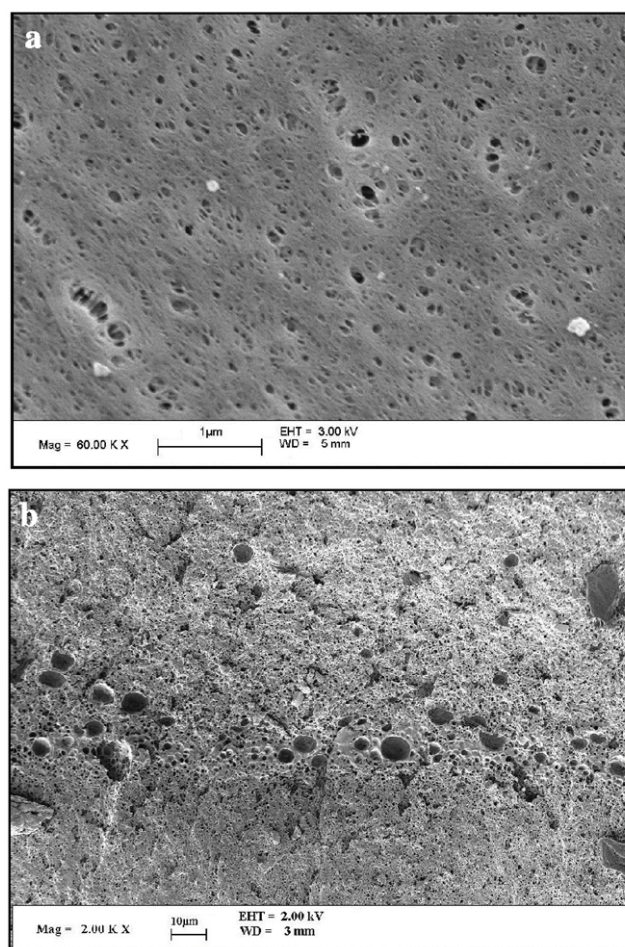


Figure 7. Morphology of cleavage surface for PMMA saturated by methanol at 60°C and then fully hydrolyzed in **a.** 60°C and **b.** 80°C distilled water.

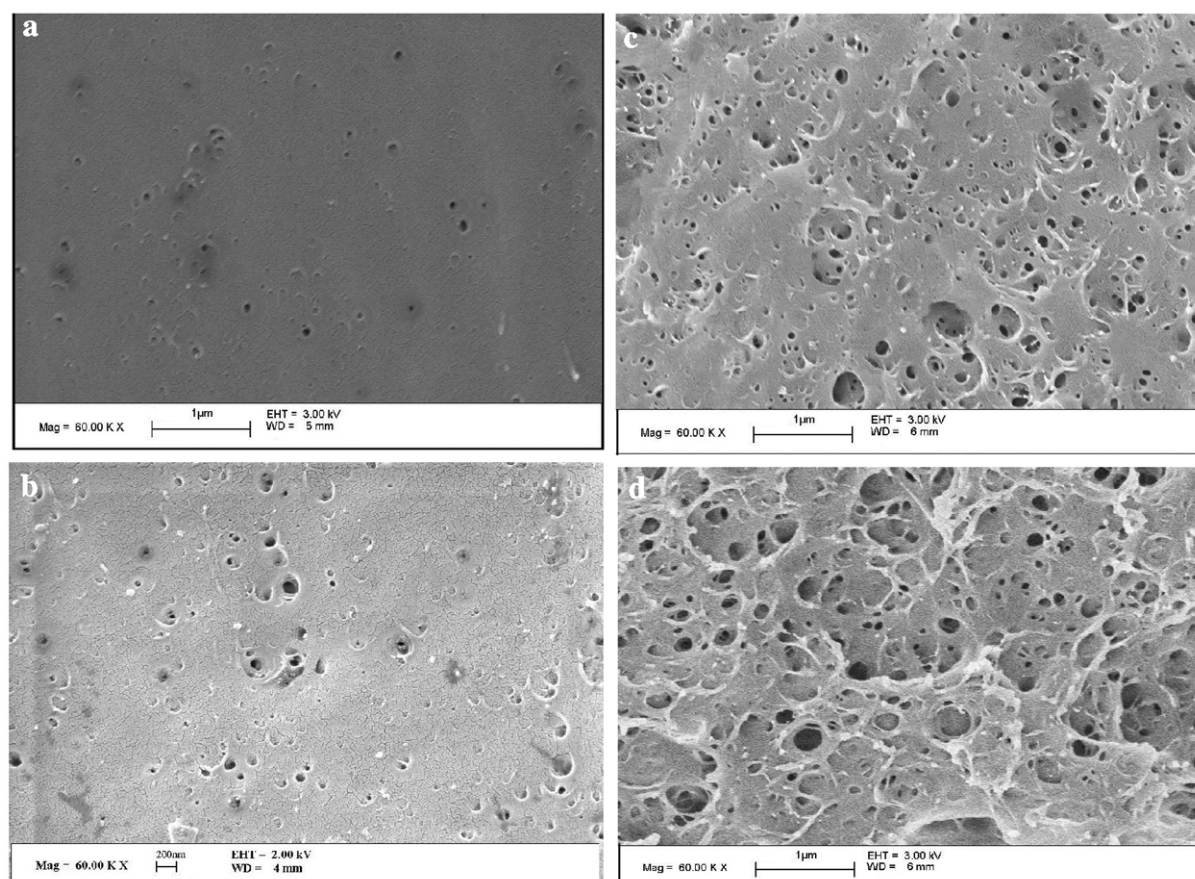


Figure 8. Morphology of PMMA specimen interior saturated by methanol at 60°C and then fully hydrolyzed in a. 50°C, b. 60°C, c. 70°C and d. 80°C distilled water.

inside the specimen to nucleate and grow and subsequently agglomerate into closed macrovoids during the hydrolysis process. In the meantime, as distilled water enters into the specimen and encounters organic solvent near the surface, co-solvent is formed, phase separation is induced and elliptic macrovoids are precipitated. The effective glass transition temperature was lowered initially when organic solvent was absorbed. Subsequently, during hydrolysis, the effective glass transition temperature gradually recovered as phase separation took place. When it elevated to above the hydrolysis temperature, the macrovoids stopped growing. Relative to hydrolysis in atmosphere, where the solvent diffused and dissipated outwardly from inside the specimen rapidly, there was not much chance for macrovoids to nucleate and grow.

3.5 Effects of hydrolysis temperature and solvent on macrovoid morphology

From table 2, both volume expansion rate and void ratio increased with increasing hydrolysis temperature. This is so because more macrovoids are formed as the hydrolysis

temperature is raised, as shown in figures 3–13. In the methanol system, table 2 shows that the volume expansion rate increases rapidly at hydrolysis temperatures, 60°C and 70°C, but it decreases slowly at 80°C, respectively. In the ethanol system, on the other hand, it increases more steeply at the lower end of the hydrolysis temperature near 40°C but starts to decrease slowly as the hydrolysis temperature gets above 70°C. The explanation is that at the steep expansion temperatures, viz. 60–70°C, for the methanol system and 40–60°C for ethanol, elliptic macrovoids are formed near the specimen surfaces that cause a sizeable change in volume. The reason elliptic macrovoids are formed is that they help mass transport of distilled water into the specimen at higher hydrolysis temperatures and at the same time inhibit the solvent from hydrolyzing out of the specimen. Therefore, the resident time of the organic solvent inside the specimen is lengthened. Co-solvent forms and agglomerates on the surface when the solvent is mass transported out of the specimen and encounters distilled water. Besides, with solvent resident time sufficiently lengthened, macrovoids have enough time to nucleate and grow. The continuous outward dissipation of organic solvent and the continuous aggregation

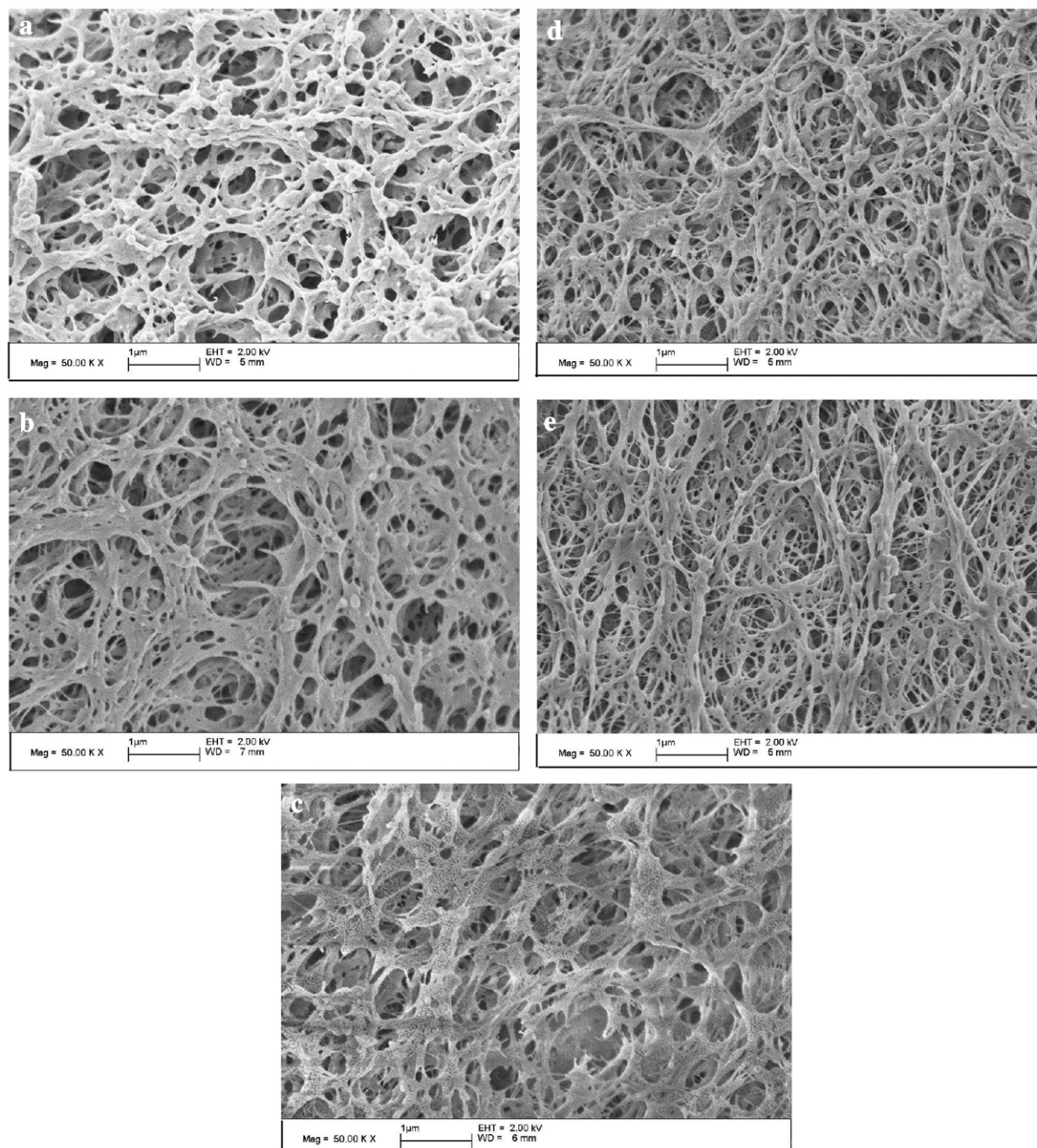


Figure 9. Magnified micrographs inside the elliptic macrovoids for PMMA saturated by methanol at 60°C and then hydrolyzed for **a.** 0.5 h, **b.** 1 h, **c.** 2 h, **d.** 3 h and **e.** 4 h.

of co-solvent near the specimen surface entail the growth process of the elliptic macrovoids. Macrovoids stop growing when the effective glass transition temperature of the polymer adjacent to the aggregate of co-solvent is elevated above the hydrolysis temperature. Since the amount of absorption is larger in the ethanol system than in methanol, and the effective glass transition temperature is lower, the amount of distilled water mass transported into the specimen and the amount of ethanol mass transported out are both larger. As a result, a larger amount of

co-solvent is aggregated and bigger elliptic macrovoids are formed in the ethanol system than in methanol. Since the speed for methanol to leave PMMA is faster than ethanol, from the standpoint of the specimen that was saturated by solvent at 60°C, hydrolysis at a lower temperature is like a cooling process. As a result, due to difference in solubility, it is not as easy for hot water to enter the specimen and to interact with the solvent in it. Few macrovoids reach critical size and shape fast enough that they shrink back slowly. On the other hand, the combined

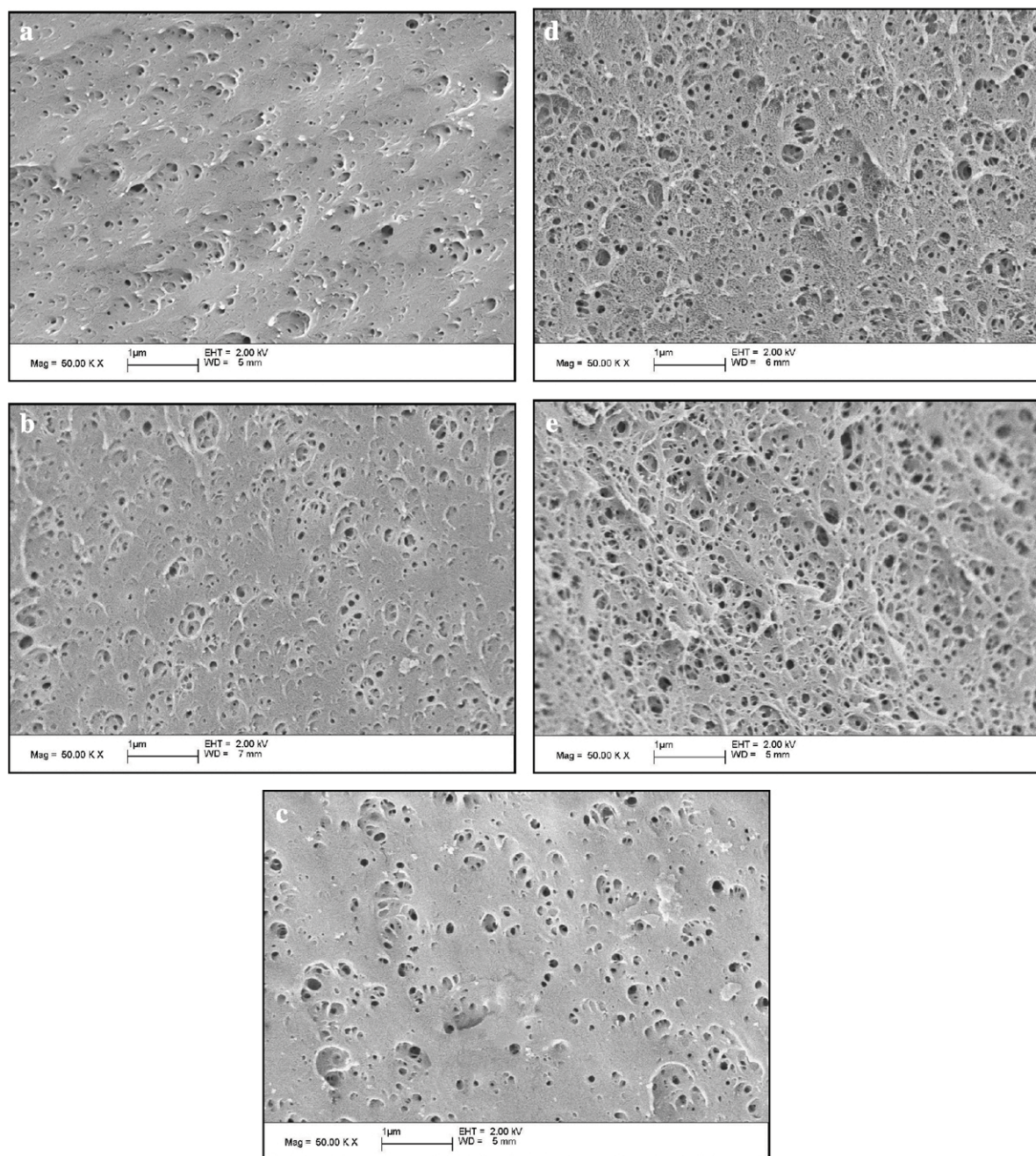


Figure 10. Morphology of the specimen interior for PMMA saturated by methanol at 60°C and then hydrolyzed for a. 0.5 h, b. 1 h, c. 2 h, d. 3 h and e. 4 h.

effect of mass transport of the organic solvent out of the specimen and mass transport of distilled water into the specimen is the decrease in concentration gradient and thus the slowdown of the hydrolysis process, causing the organic solvent to spend more time in the interior of the specimen. As a result, the chance increases for the organic solvent in the interior of the specimen to nucleate and grow, allowing more interior macrovoids to be formed.

In the methanol system, no macrovoids were detected inside the specimens at hydrolysis temperature, 40°C. Only a few closed macrovoids existed at hydrolysis temperature of 50°C. This is because at lower hydrolysis temperature, mass transport of distilled water into the specimens is not as easy, allowing easier dissipation of methanol from PMMA. The macrovoids inside the elliptic macrovoids near the surface layer at 60°C hydrolysis was

Table 2. The relationships between hydrolysis temperature and volume expansion rate, density and void ratio for PMMA after absorbing the saturated methanol and ethanol.

Solvent	Hydrolysis temperature (°C)	$(V - V_0)/V_0 \times 100\%$	$\rho \times 10^{-3} \text{ (g/mm}^2\text{)}$	$(\rho - \rho_0)/\rho_0 \times 100\%$
Methanol	40	0	1.3	0
	50	7.7	1.2	6.9
	60	30.0	1.0	23.1
	70	61.5	0.81	37.7
	80	111.7	0.61	53.2
Ethanol	40	79.6	0.72	44.6
	50	128.5	0.57	56.2
	60	145.8	0.53	59.2
	70	160.1	0.5	61.5
	80	169.9	0.48	63.1

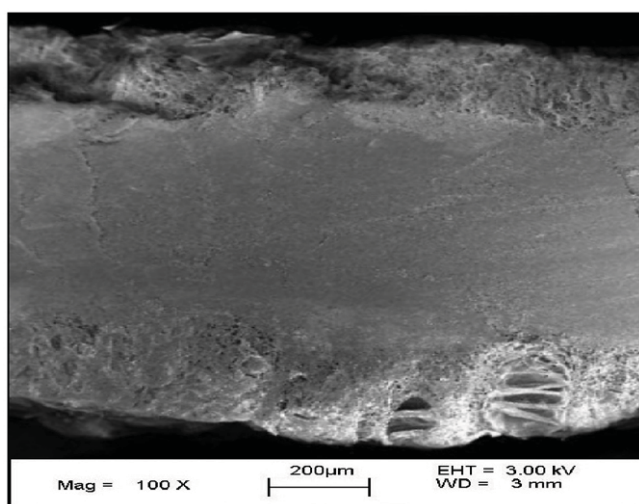


Figure 11. Cleavage surface morphology for PMMA saturated by ethanol at 60°C and completely hydrolyzed at 80°C for 3 h.

a kind of interpenetrating, web-like structure. This is because an elliptical macrovoid is a site where solvent and distilled water aggregate. For the solvent to be mass transported towards it, this site has a lower effective glass transition than its surroundings, giving it a chance to grow into an elliptical macrovoid. Elliptical macrovoids near the surface were larger at hydrolysis temperature of 70°C than at 60°C. It is because the effective glass transition temperature recovers more slowly at higher hydrolysis temperature. No aggregated elliptical macrovoids were found near the specimen surface at hydrolysis temperature, 80°C. Therefore, they are all interpenetrating macrovoid structures in the specimen interior. The reason is that, at this higher water temperature, more water goes into the membrane layer that helps enticing the solvent and water into stronger and faster phase separation interactions. As a result, distinctly different cavities are left in the specimen surface layer. At higher hydrolysis temperature, these cavities are larger in size and closer in distance between cavities. Interpenetration of the macrovoids was even

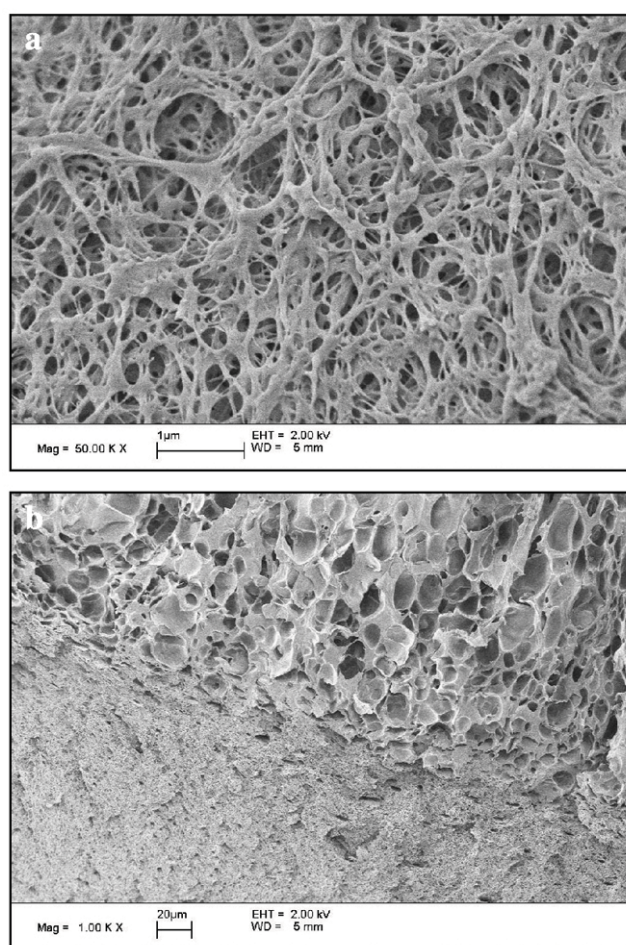


Figure 12. For PMMA saturated by ethanol at 60°C: **a.** the morphology inside the elliptical macrovoids at 60°C hydrolysis is open-type and **b.** the macrovoids at 70–80°C hydrolysis is sponge-like type.

more obvious at 90°C. This is because at 80°C, the recovery time of the effective glass transition temperature for the inner and the outer layers are almost equal. As the effective glass transition temperature recovers and goes above the

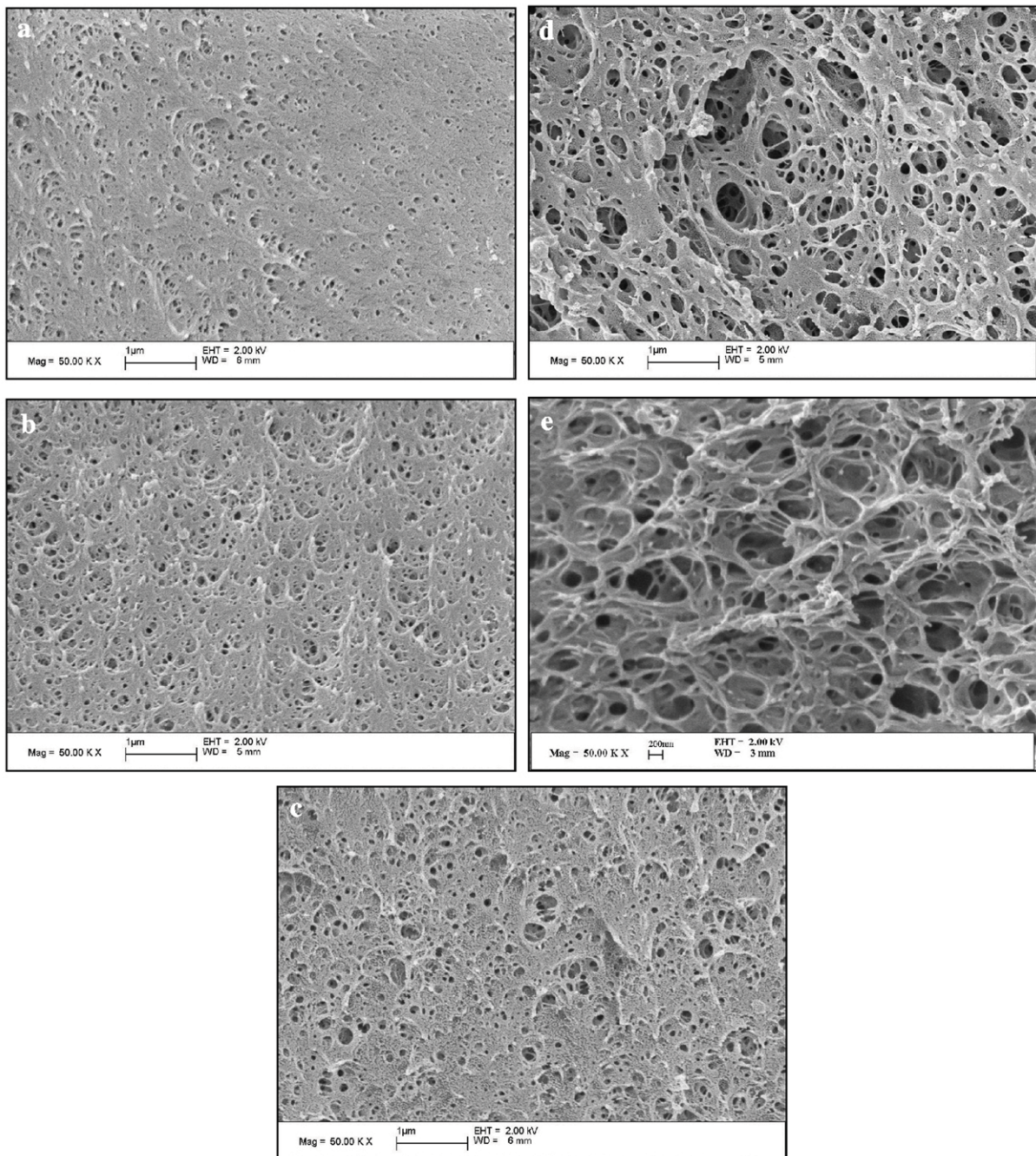


Figure 13. Micrographs inside the macrovoids for PMMA saturated by ethanol at 60°C and then fully hydrolyzed at a. 40°C, b. 50°C, c. 60°C, d. 70°C and e. 80°C.

hydrolysis temperature, a large quantity of solvent still remains inside the specimen with higher hydrolysis temperature.

3.6 Transmittance and macrovoids relationship

PMMA is an excellent light transmitter. However, they turned opaque after they absorbed methanol and ethanol

at 60°C and then hydrolyzed in distilled water from 40–80°C, as shown in figure 14. According to Lin *et al* (1991, 1992), PMMA became opaque after it absorbed methanol and then went through furnace-cooling or air-cooling. The reason is that macrovoids are formed inside the specimen during furnace-cooling or air-cooling process. Light scattering by these macrovoids reduces the amount of light transmitted, turning the specimen opaque. Figure 13(c) is the SEM morphology of the cleavage surface

Table 3. The inter-dependent relationships of $I_s = a\lambda^{-n}$ for PMMA absorbed with methanol and ethanol, by which the values of a and n in the methanol and ethanol systems can be obtained.

Solvent	Desorption temperature	40°C	50°C	60°C	70°C	80°C
Methanol	a	6.38	3.18	0.64	0.15	0.06
	n	2.83	1.38	0.28	0.07	0.04
Ethanol	a	0.41	0.39	0.31	0.08	0.03
	n	0.21	0.17	0.14	0.04	0.02

Solvent	Desorption time	0.5 h	1.0 h	2.0 h	3.0 h	4.0 h
Methanol	a	1.03	1.12	0.77	0.64	0.60
	n	0.50	0.50	0.34	0.28	0.26
Ethanol	a	0.60	0.45	0.31	0.31	0.30
	n	0.28	0.20	0.14	0.14	0.13

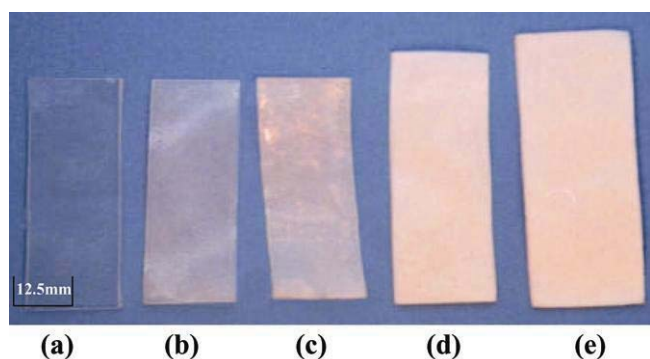


Figure 14. Micrographs for PMMA with saturated ethanol at 60°C and then fully hydrolyzed at a. 40°C, b. 50°C, c. 60°C, d. 70°C and e. 80°C.

inside a PMMA specimen that was hydrolyzed at 60°C for 3 h after it was saturated by ethanol at 60°C. The diameter of these macrovoids was about 0.13–0.55 μm . There were about 4,000,000 macrovoids per square millimeter (mm^2) and the average inter-void distance was about 0.8 μm . For furnace-cooled specimens in the above cited literatures (Lin *et al* 1991, 1992), the diameter of the macrovoids was about 5–35 μm and there were about 550 macrovoids per square millimeter (mm^2) where the average inter-void distance was about 40 μm . Comparing these two sets of data, the diameter of the macrovoids in the furnace-cooled studies was about 35 ~ 65 times larger than in the present study. This is because the recovery time of the glass transition temperature (T_g) in the furnace-cooling process is slower than the present study, allowing more time for its macrovoids to grow bigger. On the other hand, there is less amount of solvent aggregated inside each macrovoid as it takes shape in the surface layer during phase separation. Formation of macrovoids in the interior, the way they nucleate and grow, is similar to the process in furnace cooling. The solvent is mass transported into the free volumes in PMMA. Therefore, the distance between polymeric chains is increased and bonding between polymeric chains, which includes the Van der Waal force and mechanical locking, weakened.

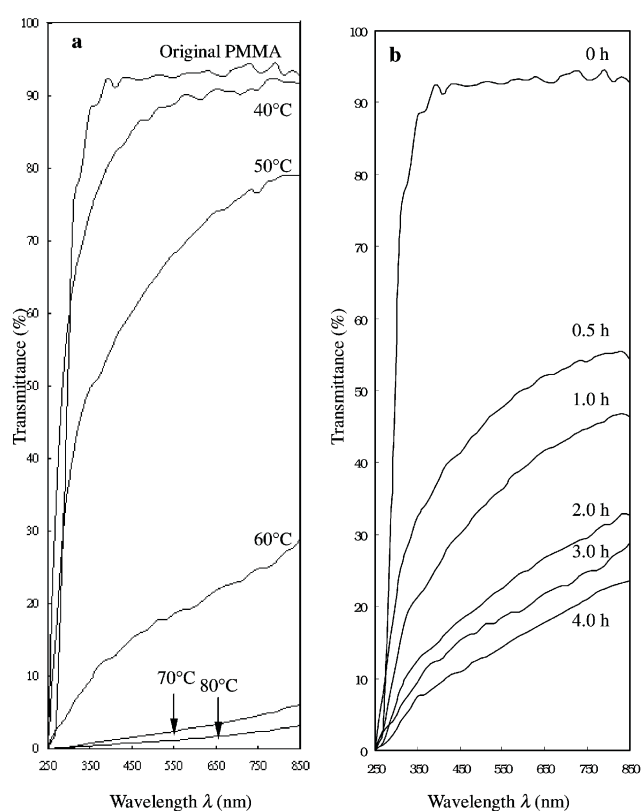


Figure 15. Relationship between transmittance and wavelength for PMMA saturated by methanol at 60°C and then hydrolyzed at various hydrolysis a. temperatures and b. times.

The effective glass transition temperature ($T_{g\text{eff}}$) is thereby lowered, causing plasticization and swelling. After solvent enters and expands the macrovoids, these macrovoids do not completely shrink back during atmospheric hydrolysis. Therefore, when $T_{g\text{eff}}$ recovers to its original temperature (104°C), the spaces originally filled with solvent become macrovoids that are light scattering. (It is similar to the growth in metallic crystals in which the small-sized crystals become smaller and the large-sized crystals grow larger.) According to Rayleigh's study on light scattering of micro particles, which became Rayleigh's law of scattering

as was proposed in 1871, the scattering light intensity is inversely proportional to the wavelength of the incident light to the 4th power (15), i.e.:

$$I \propto \frac{1}{\lambda^4}, \quad (4)$$

where I is the scattering light intensity, λ the wavelength of the incident light.

When light enters a PMMA specimen, besides directly passing through, it can also go through unlimited rounds of reflection and scattering by macrovoids of irregular surface contours along its path. A reflected beam can be considered as another incident light beam. The smaller the inter-void distance is, the stronger the scattering intensity, and the resultant opacity becomes more obvious. Applying the above equation, the ratio of scattering intensity is about 16 for the specimen in the present study. But the ratio of scattering intensity for the furnace-cooled specimen was only about 3.9×10^{-7} .

The transmittance to wavelength relationship at various hydrolysis temperatures and times for PMMA saturated by methanol and ethanol before fully hydrolyzed in distilled water are shown in figures 15 and 16, respectively. As can be seen, transmittance decreased with increasing

hydrolysis temperature and time. Figures 17 and 18 show the corresponding plots in logarithm scale where the scattering intensity to wavelength relationship is linear. Adopting the more generalized formula form, $I_s = a\lambda^{-n}$, we can find the a and n values, respectively, based on experimental data for the methanol and ethanol systems, as shown in table 3. It is deducible that, for the methanol system, since more elliptic macrovoids were formed in the skin layer and since there were more macrovoids inside each elliptic macrovoid at 60°C, there are more intense multi-layer scattering than at 50°C, resulting in a lower transmittance at 60°C than at 50°C. Similarly, the same effect is deducible for the ethanol system.

4. Conclusions

The conclusions are summarized as follows:

(I) For PMMA specimens pre-saturated by solvent and then hydrolyzed in distilled water, the weight of the specimen increases with both the hydrolysis time and the hydrolysis temperature. The amount of weight gained is greater in ethanol systems than in methanol.

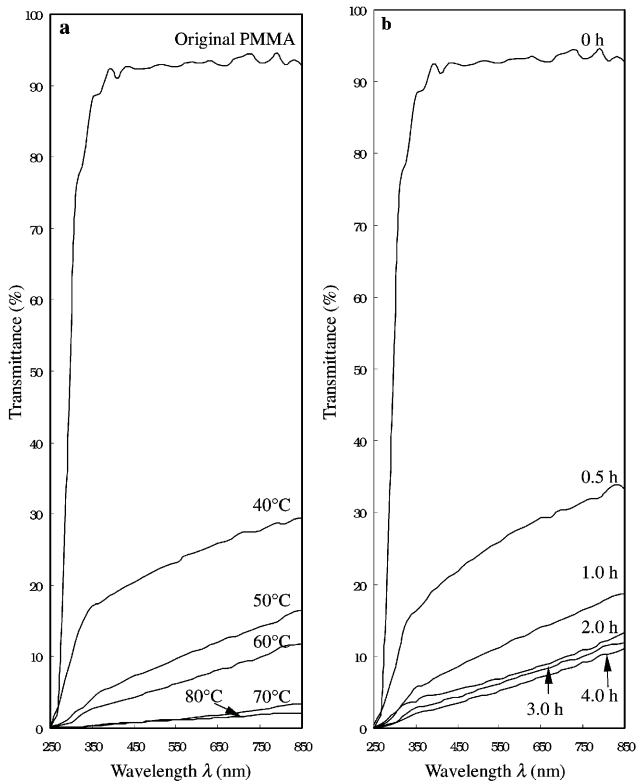


Figure 16. Relationship between transmittance and wavelength for PMMA saturated by ethanol at 60°C and then hydrolyzed at various hydrolysis a. temperatures and b. times.

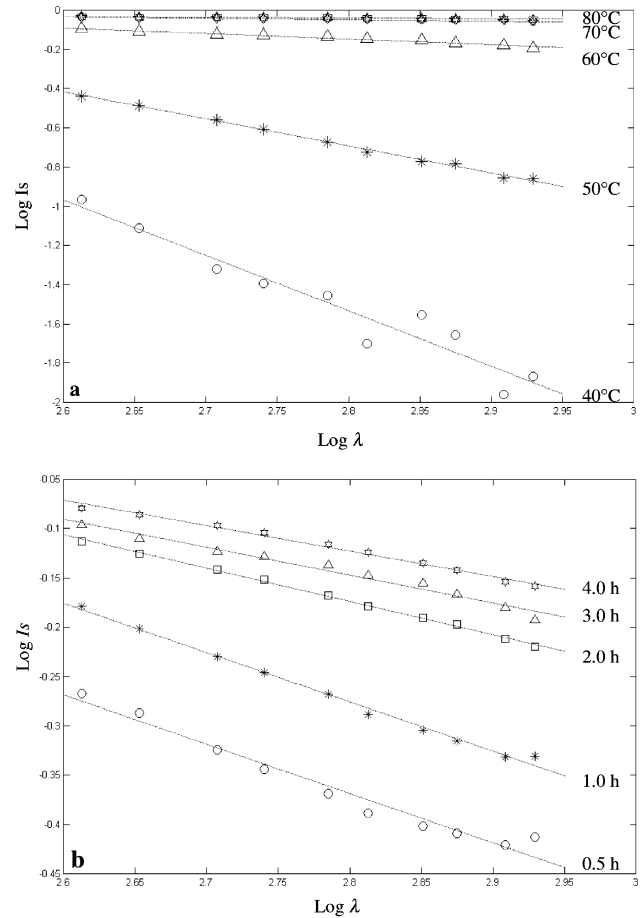


Figure 17. Same as in figure 15 except in logarithm scale.

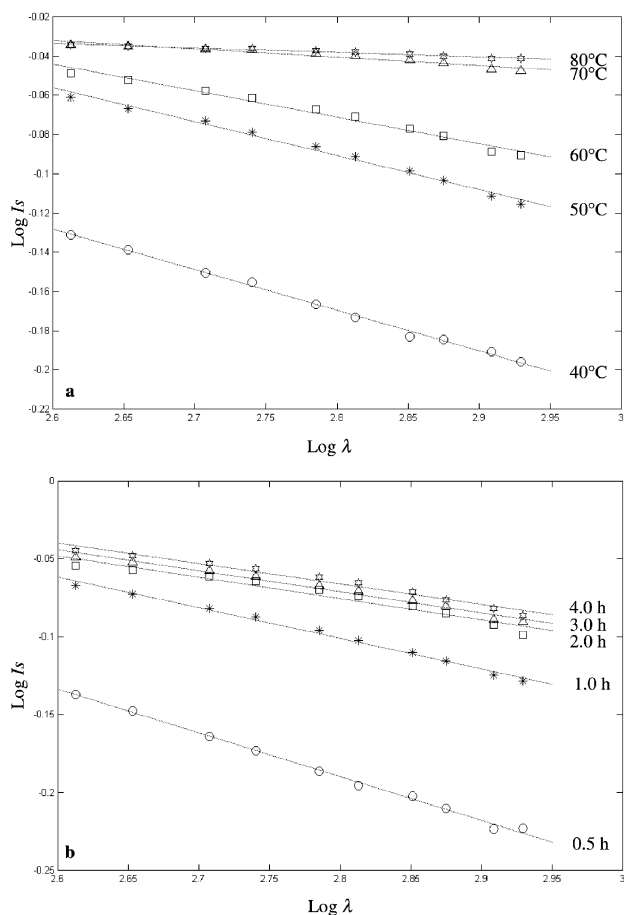


Figure 18. Same as in figure 16 except in logarithm scale.

(II) In methanol systems, elliptic macrovoids are formed in the skin layer after hydrolysis at 60°C distilled water. And there are closed-type macrovoids inside these elliptic

macrovoids. Sponge-like macrovoids are formed in the outside layer at 80°C. Macrovoids in the interior region of the specimen are all closed-type and their size and number increase with both the hydrolysis temperature and the hydrolysis time, except at 80°C, where they are open-type instead.

(III) In ethanol systems, elliptic macrovoids are formed in the skin layer at hydrolysis temperature, 40–60°C in distilled water. Inside these elliptic macrovoids are open-type macrovoids whose size and number increase with hydrolysis time. At 70–80°C, macrovoids in the skin layer are sponge-like. In the interior of the specimen, the macrovoids are closed-type from 40–60°C and open-type from 70–80°C.

(IV) Transmittance of the specimens decreases due to light scattering effect of the macrovoids. The loss in transmittance increases with both the hydrolysis temperature and time and the loss is more apparent in ethanol systems than in methanol.

References

- Buczkowski S, Hildgen P and Cartilier L 1998 *Fractals* **6** 171
 Chou K F and Lee S 2000 *Polymer* **41** 2059
 Harmon J P, Lee S and Li J C M 1987 *J. Polym. Sci. Part A: Polym. Chem. Ed.* **25** 3215
 Harmon J P, Lee S and Li J C M 1998 *Polymer* **29** 1221
 Jenkins F A and White H E 1950 in *Fundamentals of optics* (New York: McGraw-Hill) 2nd edn, Ch. 22
 Lin C B, Liu K S and Lee S 1991 *J. Polym. Sci.: Part B: Polym. Phys.* **29** 1457
 Lin C B, Liu K S and Lee S 1992 *J. Appl. Polym. Sci.* **44** 2213
 Orbach R 1986 *Science* **231** 814
 Wong P Z 1985 *Phys. Rev.* **B32** 7417